Very long chain n-3 and n-6 polyunsaturated fatty acids bind strongly to liver fatty acid-binding protein

Andrew W. Norris[1,*] **and Arthur A. Spector**[†]

Department of Pediatrics* and Department of Biochemistry,[†] University of Iowa College of Medicine, Iowa City, IA 52242

Abstract **Synthesis of n-3 and n-6 very long chain-PUFAs (VLC-PUFAs) from 18-carbon essential fatty acids is differentially regulated. The predominant product arising from n-3 fatty acids is docosahexaenoic acid (22:6n-3), with the liver serving as the main site of production. The synthetic pathway requires movement of a 24-carbon intermediate from the endoplasmic reticulum to peroxisomes for retroconversion to 22:6n-3. The mechanism of this intra-organelle flux is unknown, but could be binding-protein facilitated. We thus investigated binding of a series of previously untested VLC-PUFAs to liver fatty acid-binding protein (L-FABP). Three fluorometric assays were employed, all of which showed strong binding (K_d' ~10^{-8} to 10^{-7} M) of 20-, 22-, and 24-carbon n-3 PUFAs to L-FABP. In contrast, synthesis of the predominant n-6 PUFA product, arachidonic acid, does not require intra-organelle transport. However, we found that n-6 VLC-PUFAs bound to L-FABP with affinities (K_d' ~10^{-8} to 10^{-7} M) comparable to their n-3 counterparts. Although these results raise the possibility that L-FABP may participate in the cytoplasmic processing of n-3 and n-6 VLC-PUFAs, there is no evidence on the basis of binding affinities that L-FABP accounts for differences in the predominant products formed by the n-3 and n-6 PUFA metabolic pathways.**—Norris, A. W., and A. A. Spector. **Very long chain n-3 and n-6 polyunsaturated fatty acids bind strongly to liver fatty acid-binding protein.** ***J. Lipid Res.*** **2002.** 43: **646–653.**

Supplementary key words 24-carbon polyunsaturated fatty acids • docosahexaenoic acid • arachidonic acid • fatty acid binding assay

In humans, n-3 and n-6 PUFAs cannot be synthesized and must be obtained from dietary sources, predominantly in the form of 18:2n-6 (linoleic acid) and 18:3n-3 (linolenic acid) (1–3). These 18-carbon PUFAs are then processed enzymatically to specific very long chain-PUFAs (VLC-PUFAs). The predominant n-6 PUFA end-product is 20:4n-6 (arachidonic acid), which is essential as the substrate for eicosanoid metabolism. The predominant n-3 PUFA end-product is 22:6n-3 (docosahexaenoic acid), which is essential for visual and neurological development (4–6). In addition, 22:6n-3 may be critical for normal function of other tissues, as evidenced by the ability of 22:6n-3 to improve pathologic findings in lung, pancreas, and ileum of the *cftr*$^{-/-}$ mouse (7), and to improve liver abnormalities in persons with low 22:6n-3 levels secondary to Zellweger syndrome (6). There also is evidence that 22:6n-3 may modulate nuclear signaling through binding to the retinoid X receptor (8).

The main site of 18:3n-3 to 22:6n-3 conversion is the liver, and 22:6n-3 is then circulated to brain and retina where it accumulates. The metabolic pathway through which 18:3n-3 is converted to 22:6n-3 starts in the endoplasmic reticulum with several elongation and desaturation steps, producing 24:6n-3 (1). The 24:6n-3 is then transported by an unknown mechanism to peroxisomes for retroconversion to 22:6n-3 (1), illustrated 18:3n-3 → 18:4 → 20:4 → 20:5 → 22:5 → 24:5 → 24:6 ⇒ **22:6**, where bold type indicates the predominant fatty acid product, and the open arrow represents the enzymatic step that occurs in the peroxisome. The 22:6n-3 thus formed is then transported from the peroxisomes back to the endoplasmic reticulum for esterification into phospholipids.

Although n-6 PUFAs also can be processed through the entire VLC-PUFA pathway, the predominant end product in most tissues under ordinary circumstances is 20:4n-6 (arachidonic acid). Only a small fraction continues to 22:4n-6, and virtually none ordinarily continues to 24 carbon intermediates (1), illustrated 18:2n-6 → 18:3 → 20:3 → **20:4** → 22:4 → 24:4 → 24:5 ⇒ 22:5, where small arrows indicate steps that ordinarily are less active. Only in a state of n-3 PUFA deficiency is a substantial amount of n-6 PUFA converted to 24–carbon intermediates for peroxisomal retroconversion to 22:5n-6 (2). The mechanisms responsible for the differential control of n-3 and n-6 PUFA metabolism are unknown.

Liver fatty acid-binding protein (L-FABP) is a member of the family of small, intracellular proteins that bind lipids with high affinity (9, 10). It is highly expressed in liver, accounting for up to 5% of cytoplasmic protein. There is evi-

Abbreviations: ANS, 8-anilino-1-naphthalenesulfonate; DAUDA, 11-[(5–dimethylaminonaphthalene-1-sulfonyl)amino]undecanoic acid; L-FABP, liver fatty acid-binding protein; VLC-PUFA, very long chain-polyunsaturated fatty acid.

[1] To whom correspondence should be addressed at Joslin Diabetes Center, Cellular and Molecular Physiology, One Joslin Place, Boston, MA 02215.
e-mail: andrew.norris@joslin.harvard.edu

dence that FABPs may influence fatty acid metabolism through facilitating uptake, transport, sequestration, and/or metabolic targeting of fatty acids (11, 12). Overexpression of L-FABP in fibroblasts stimulates cellular uptake of fatty acid and esterification of fatty acid into specific lipid classes (13, 14). L-FABP may thus direct transport of fatty acids to various cellular targets (15). For example, recent evidence suggests that complexes of fatty acid and L-FABP interact specifically with the nucleus and nuclear proteins (16). L-FABP differs from other FABPs in that it binds two, rather than one, fatty acids in its large binding pocket, which is also capable of binding a variety of other hydrophobic ligands, including fatty acyl CoA esters, heme, oxygenated fatty acids including eicosanoids, and bilirubin (10, 17, 18). Of VLC-fatty acids, L-FABP has been shown to bind 20:4n-6, 22:6n-3, and 24:1n-9 with sub-micromolar affinities (15, 17–19), though binding of no other VLC-PUFAs to L-FABP or other FABPs has been investigated.

The purpose of the present study was to determine whether L-FABP might participate in control of VLC-PUFA processing by preferential binding to intermediate PUFAs in the n-3 and n-6 pathways. To evaluate this possibility we investigated the binding of a series of n-3 and n-6 VLC-PUFAs to L-FABP using three fluorescence based binding assays.

MATERIALS AND METHODS

Materials

The fluorescently labeled fatty acid 11-[(5–dimethylaminonaphthalene-1-sulfonyl)amino]undecanoic acid (DAUDA) was obtained from Molecular Probes (Eugene, OR). 8-anilino-1-naphthalenesulfonate (ANS) ammonium salt was from Fluka. Gelatin (product G-2500) and docosahexaenoic acid (22:6n-3, product D2534) were obtained from Sigma Aldrich (St. Louis, MO). The 24 carbon VLC-PUFAs (24:4n-6, 24:5n-6, 24:5n-3, and 24:6n-3), dissolved in ethanol, were a kind gift from Dr. Howard Sprecher (Ohio State University). The remaining PUFAs were obtained from Cayman Chemical (Ann Arbor, MI). All PUFAs were stored at –20°C or less, under N_2. The fluorescence probes were dissolved in ethanol, and quantitated by absorbance spectroscopy using ε_{334nm} = 4,500 cm^{-1} M^{-1} for DAUDA (lot specific data sheet) and ε_{372nm} = 8,000 cm^{-1} M^{-1} for ANS (20).

L-FABP

Delipidated recombinant rat L-FABP (21, 22) was a kind gift from Dr. Friedhelm Schroeder (Texas A&M University). The concentration of L-FABP was determined by quantitative amino acid analysis. Measurement of the absorbance at 280 nm of the quantitated sample yielded an extinction coefficient of 6,370 cm^{-1} M^{-1}, near that determined by Thompson et al. (23) of 6,400 cm^{-1} M^{-1}.

Fluorescence measurements

Steady state fluorescence was measured at 25°C using a fluorometer (Fluorolog, Instruments S.A., Inc., Edison, NJ) with 1 cm pathlength cuvettes, temperature jacket, sample stirring, 1 s integration time, and reference normalization. All titrations were performed in 20 mM KPO_4, pH 7.4, 100 mM KCl.

Titrations measuring intrinsic L-FABP fluorescence

The fluorometer excitation and emission wavelengths were set to 280 nm and 350 nm with slit widths of 2 and 5 nm, respectively. Cuvettes were equilibrated with buffer containing 0.01% gelatin, which stabilizes the fluorescence signal generated from low concentrations of protein (24). L-FABP was added to a final concentration of 450 nM, a concentration chosen as low as possible, maintaining an acceptable signal to noise ratio. The sample was titrated with fatty acid dispensed from a Hamilton syringe. For each titration point, ten seconds of fluorescence signal data were averaged and the standard error determined. The final concentration of ethanol typically did not exceed 0.7% (v/v). Control titrations were performed in the same manner except that L-FABP was omitted.

Titrations measuring displacement of competitor ligand

For ANS based experiments, the fluorometer excitation and emission wavelengths were set to 370 nm and 475 nm, respectively, with slit widths of 2 nm. Cuvettes were equilibrated with buffer containing 0.01% gelatin. L-FABP was added to a final concentration of 60 nM. ANS was then added to a final concentration of 950 nM. The sample was titrated with fatty acid and the signal averaged as described above. The final concentration of ethanol typically did not exceed 0.7% (v/v). Titrations employing DAUDA rather than ANS were performed in the same manner except that the excitation and emission wavelengths were set to 360 nm and 490 nm, respectively, the L-FABP concentration was 30 nM, and DAUDA was used at a concentration of 530 nM.

Analysis of intrinsic fluorescent binding data

L-FABP is able to bind two molecules of fatty acid, the first with high affinity and the second with lower affinity. Because these two fatty acids are located sequentially within the barrel-shaped binding cavity (10, 23), we used a sequential model of binding where the first site is occupied before the second fatty acid can bind. This can be noted symbolically as:

$$P + FA \overset{K_1}{\leftrightarrow} PFA_1 \qquad \textit{(Eq. 1)}$$

$$PFA_1 + FA \overset{K_2}{\leftrightarrow} PFA_1FA_2 \qquad \textit{(Eq. 2)}$$

where P stands for the unbound L-FABP, FA stands for unbound fatty acid, PFA_1 stands for L-FABP complexed with fatty acid in position one, and PFA_1FA_2 stands for L-FABP complexed with fatty acids in positions one and two. The mass-law and conservation-of-mass equations describing these two equilibria are:

$$K_1 = \frac{[PFA_1]}{[P] \times [FA]} \qquad \textit{(Eq. 3)}$$

$$K_2 = \frac{[PFA_1FA_2]}{[PFA_1] \times [FA]} \qquad \textit{(Eq. 4)}$$

$$P_T = [P] + [PFA_1] + [PFA_1FA_2] \qquad \textit{(Eq. 5)}$$

$$FA_T = [FA] + [PFA_1] + 2[PFA_1FA_2] \qquad \textit{(Eq. 6)}$$

where P_T is the total concentration of L-FABP in the sample, and FA_T is the total concentration of fatty acid. Following the general approach of Eftink (25), these equations can be rewritten and solved in terms of K_1, K_2, P_T, and FA_T starting with the following cubic equation whose real root defines [FA]:

$$K_1K_2[FA]^3 + (K_1 + 2K_1K_2P_T - K_1K_2FA_T)[FA]^2 + (1 + K_1P_T - K_1FA_T)[FA] - FA_T = 0 \qquad \textit{(Eq. 7)}$$

This can be used to determine the concentration of the following species:

$$P = P_T / (1 + K_1[FA] + K_1K_2[FA]^2) \quad \textit{(Eq. 8)}$$

$$[PFA_1] = K_1[P][FA] \quad \textit{(Eq. 9)}$$

$$[PFA_1FA_2] = K_2[PFA_1][FA] \quad \textit{(Eq. 10)}$$

Having normalized the initial fluorescence to 100%, the binding curve would thus take the form:

$$F = 100 + F_1[PFA_1] + F_2[PFA_1FA_2] \quad \textit{(Eq. 11)}$$

where F is the normalized fluorescence signal, and F_1 and F_2 are the molar-scaled changes in fluorescence associated with the transition from the unliganded to the first and second liganded states respectively.

Thus, knowing FA_T and P_T for the titration points, the corrected, normalized data was fit to equations 7–11 to determine the parameters K_1, K_2, F_1, and F_2. This was done using the nonlinear, least-squares regression package Scientist (MicroMath, UT). Dissociation constants, the inverse of the determined association constants, are reported as a matter of convention.

Analysis of displacement binding data

Under the conditions used in these studies where total concentration of fluorophore is much greater than that of the macromolecule, the presence of the fluorophore does not increase the complexity of the titration curves with competing ligand (18, 26). This is because the unbound fluorophore concentration essentially does not change during the titration. The low concentration of fatty acid and protein used in the displacement studies does not populate the weaker, second binding site to any appreciable degree. Thus, the titration data were fit to a simple single-site binding equation (18) using the non-linear regression package Scientist.

RESULTS

Binding of n-3 VLC-PUFAs to L-FABP measured by intrinsic fluorescence

The intrinsic fluorescence of L-FABP showed saturable reduction when titrated with n-3 VLC-PUFAs. Control titrations in the absence of L-FABP showed various increases in fluorescence, as shown in **Fig. 1**. Because PUFAs are not fluorescent at the wavelengths used in these studies, this represents trace contamination of the ligand preparations. To correct for the contaminant fluorescence, as shown in Fig. 1, backgrounds were fit to second-degree polynomials and were then subtracted from the relevant titration curves. The level of fluorescent contaminant varied between ligand preparations, with the lowest level present in 20:5n-3, an intermediate level in 24:6n-3, and higher levels in 22:5n-3, 22:6n-3, and 24:5n-3. The resultant corrected data were well described by a two-site model of sequential binding, as shown in **Fig. 2**, and typically were not as well fit with a single-site binding model. This allowed determination of the apparent binding affinity for the first (i.e., strong) binding site. A range of binding affinities of fatty acids for the second site has been reported ~0.5–30 μM (15, 27). These values predict a low-level population of the second site under the condition used in these titrations. In concordance with this prediction, the binding affinities for the second site were poorly determined under these conditions.

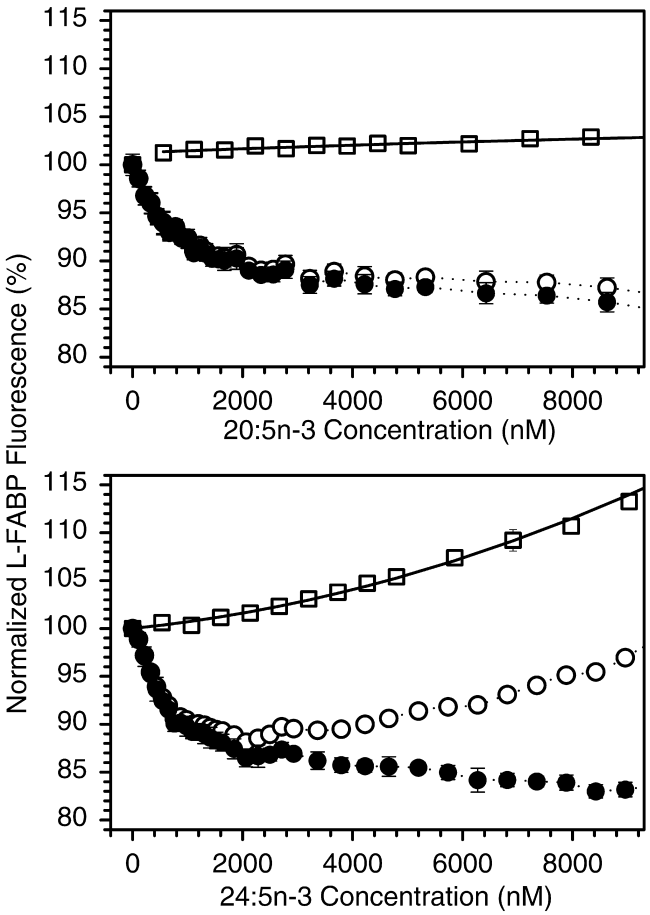

Fig. 1. Correction of contaminant fluorescence in PUFA preparations under conditions used for measurement of intrinsic liver fatty acid-binding protein (L-FABP) fluorescence. Top panel shows a PUFA preparation with minimal contaminant fluorescence, 20:5n-3; bottom panel shows the n-3 PUFA preparation with the largest contaminant fluorescence, 24:5n-3. Open circles show titration in the presence of 450 nM L-FABP. Titration in the absence of protein (open squares) shown on the same normalized scale demonstrates the degree of contaminant. Quadratic fit to the background is shown by solid line. Closed circles represent data after correction for fitted backgrounds. Bars show the standard error of the fluorescence measurements.

Binding of fluorescent probes ANS and DAUDA to L-FABP

The fluorescent probe ANS showed large, saturable increases in fluorescence upon titration into L-FABP (**Fig. 3**), whereas control titration in the absence of protein showed minimal fluorescence. The resultant data were well described by a single binding site model with a K_d of 3,400 nM (95% rigorous, support-plane confidence interval 2,900–4,000). Likewise, the fluorescent probe DAUDA showed increases in fluorescence upon titration into L-FABP (Fig. 3), though control titration in the absence of protein showed fluorescence increases. The data were

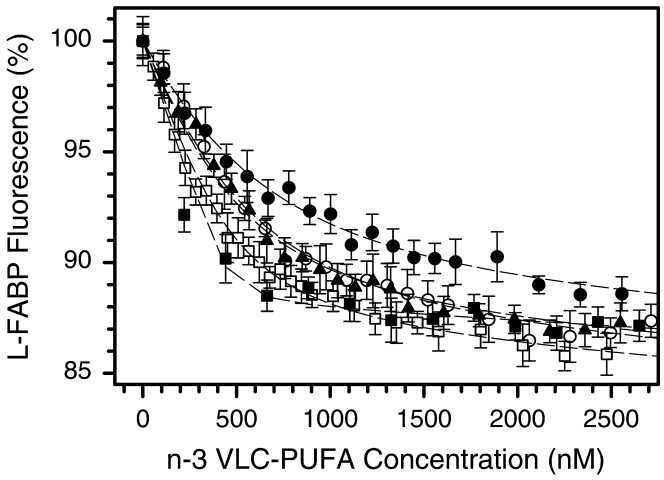

Fig. 2. Titration of 450 nM L-FABP with n-3 very long chain-polyunsaturated fatty acids (VLC- PUFAs), monitoring changes in intrinsic L-FABP fluorescence upon titration with 20:5n-3 (closed circle), 22:5n-3 (open square), 22:6n-3 (closed square), 24:5n-3 (open circle), and 24:6n-3 (closed triangle) after correction for contaminant fluorescence. Dashed lines represent non-linear regression fits used to determine binding affinities. Bars show the standard error of the fluorescence measurement.

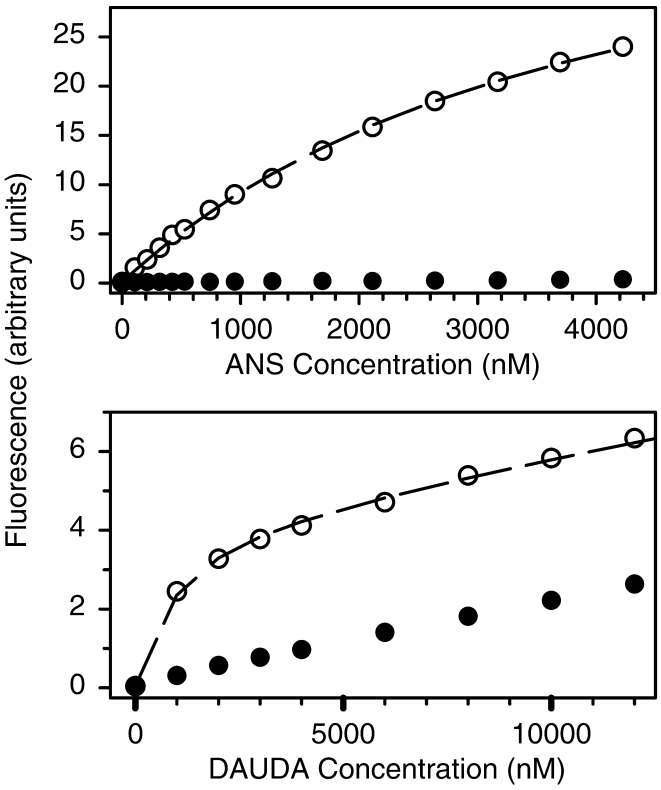

Fig. 3. Titration of L-FABP with fluorophores 8-anilino-1-naphthalenesulfonate (ANS) (top panel) and 11-[(5–dimethylamino-naphthalene-1-sulfonyl)amino]undecanoic acid (DAUDA) (bottom panel). Titration in the presence (open circle) and absence (closed circle) of protein is shown. ANS titration contained 590 nM L-FABP and DAUDA titration contained 450 nM L-FABP. Dashed line is non-linear regression to a single-site binding model. In the case of the DAUDA titration, a term for fluorescence of free fluorophore was included in the model. Bars showing the standard error of the fluorescence measurements are present, but generally smaller than the figure symbols.

therefore fit to a single binding site model with a term added to allow for fluorescence of free unbound ligand [i.e., F = F_u × (unbound DAUDA) + F_b × (bound DAUDA)]. This approach yielded a good fit, showing that DAUDA binds to L-FABP more strongly than ANS, with a K_d of 700 nM (460–1,000).

Binding of n-3 VLC-PUFAs to L-FABP measured by displacement of ANS

Titration of fatty acid into a mixture of L-FABP and ANS led to saturable decreases in ANS fluorescence, consistent with displacement of ANS from L-FABP by the fatty acid. As shown in **Fig. 4**, the resultant displacement curves were well described by a single-site model of binding. There was no discernable contaminant fluorescence, as detected by carrying titrations beyond saturation, except for slight amounts in 24:5n-3. Approaches to correct for this minimal background did not change the resultant modeled affinities. The binding affinities determined by the various fluorescence approaches are shown as apparent association constants in **Fig. 5** to allow comparison of the different methods.

Binding of n-3 VLC-PUFAs to L-FABP measured by displacement of DAUDA

Just as for ANS, titration of fatty acid into a mixture of L-FABP and DAUDA led to saturable decreases in DAUDA fluorescence, consistent with displacement of DAUDA from L-FABP by the fatty acid. There was no discernable contaminant fluorescence, except for slight amounts in 24:5n-3. Approaches to correct for this minimal background did not change the resultant modeled affinities. As with ANS, data were well described by the simple single-site binding equation, as shown in **Fig. 6**. Figure 5 shows the calculated binding constants.

Binding of n-6 VLC-PUFAs to L-FABP

Like n-3 VLC-PUFAs, titration of L-FABP with n-6 VLC-PUFAs resulted in saturable decreases in intrinsic fluorescence which were well described by a two-site model of sequential binding, as shown in **Fig. 7**. Minimal contaminant fluorescence was present in the 20:4n-6 and 22:4n-6 preparations, with a larger amount in the 24:4n-6 preparation. The 24:5n-6 preparation had very large fluorescence contamination, 6–8 times that of 24:5n-3 and 24:4n-6.

As also shown in Fig. 7, n-6 VLC-PUFAs were able to displace both ANS and DAUDA, with good fits of the data to a single-site binding model. There was no discernable contaminant fluorescence, except for 24:5n-6, and a slight amount in 24:4n-6. Approaches to correct for these minimal backgrounds did not change the resultant modeled affinities. The calculated binding constants for these data also are shown in Fig. 5.

Overall, the ANS based assay benefits from the advantage of a weaker competitor fluorophore and greater fluorescence enhancement compared with DAUDA, as well as the ability to study much lower protein concentrations

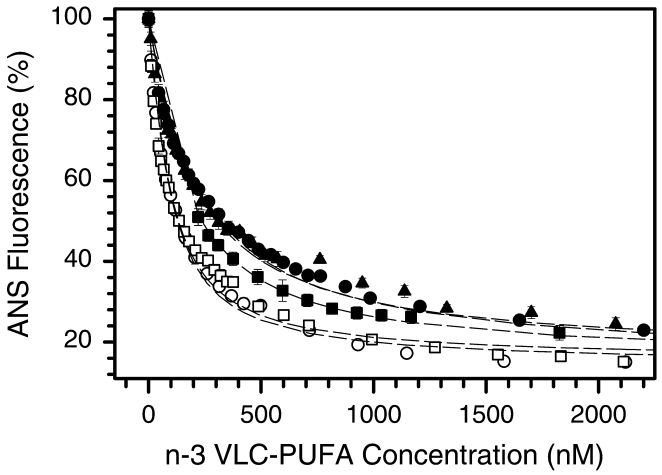

Fig. 4. Titration of 60 nM L-FABP containing 950 nM ANS with n-3 VLC-PUFAs, monitoring ANS fluorescence upon titration with 20:5n-3 (closed circle), 22:5n-3 (open square), 22:6n-3 (closed square), 24:5n-3 (open circle), and 24:6n-3 (closed triangle). Dashed lines represent non-linear regression fits used to determine binding affinities. Bars showing the standard error of the fluorescence measurement are present, but generally smaller than the figure symbols.

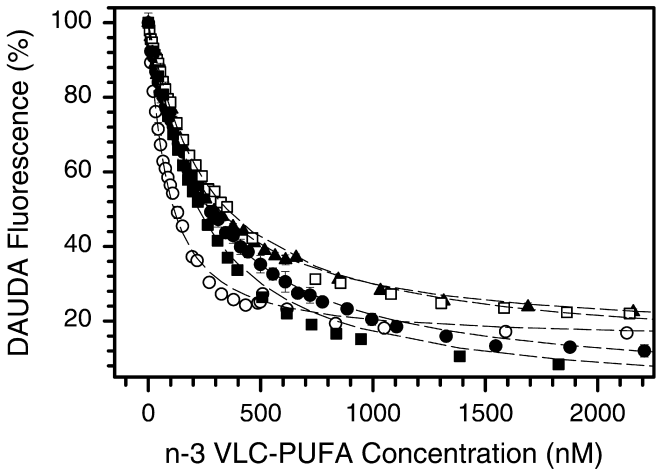

Fig. 6. Titration of 30 nM L-FABP containing 530 nM DAUDA with n-3 VLC-PUFAs, monitoring DAUDA fluorescence upon titration with 20:5n-3 (closed circle), 22:5n-3 (open square), 22:6n-3 (closed square), 24:5n-3 (open circle), and 24:6n-3 (closed triangle). Dashed lines represent non-linear regression fits used to determine binding affinities. Bars showing the standard error of the fluorescence measurement are present, but generally smaller than the figure symbols.

compared with the intrinsic fluorescence studies. For these reasons the ANS assay likely best represents the binding of VLC-PUFAs to L-FABP. The apparent binding constants determined by the ANS assay are presented in **Table 1** to allow comparison of n-3 and n-6 VLC-PUFA binding to L-FABP. Both n-3 and n-6 VLC-PUFAs were found to bind strongly to L-FABP, with K_d's ranging from 7–200 nM.

DISCUSSION

Three fluorescence based assays of PUFA binding to L-FABP

Two of the assays we employed measured binding of n-3 and n-6 VLC-PUFAs to L-FABP by monitoring displacement of competitor fluorescent ligands. The fluorophore ANS is ideally suited for this (18, 20), as it binds relatively weakly to L-FABP and has a large enhancement of its fluorescence in the bound state. DAUDA has the same attributes as ANS, though it binds more strongly to L-FABP and thus will perturb the equilibrium to a larger degree. It also has a larger relative fluorescence signal in the unbound state than ANS. Because ANS, compared with DAUDA, binds more weakly to L-FABP, the determined apparent affinities are expected to be somewhat stronger. This will be offset to some degree in these studies, because the concentration of ANS was higher than that of DAUDA. Thus, under these conditions, the affinities determined by ANS should be slightly stronger than those determined by DAUDA. In accord with this expectation, there was a trend toward slightly stronger affinities determined by ANS (Fig. 5). Because of the advantages mentioned above, we believe that the ANS based assay best represents the binding of VLC-PUFAs to L-FABP. Indeed, a similar ANS based study of fatty acid binding to FABP showed comparable results when directly tested against an established assay (18) employing acrylodan labeled intestinal fatty acid binding protein (ADIFAB).

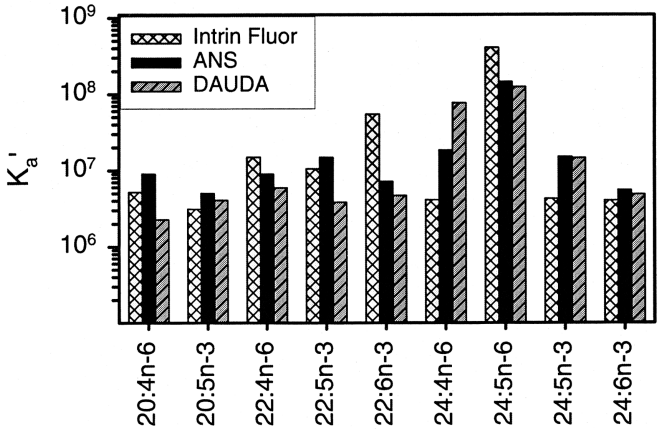

Fig. 5. Apparent association constants of VLC-PUFA binding to L-FABP as determined by the intrinsic fluorescence (cross hatched, light gray), ANS displacement (solid black), and DAUDA displacement assays (medium gray, side hatched).

Because L-FABP does not have tryptophan residues, unlike many other FABPs, its intrinsic fluorescence signal likely comes predominately from its three tyrosine residues, all of which line the binding cavity (10). Alteration of tyrosine fluorescence upon lipid binding has been described for other proteins (28). The intrinsic fluorescence assay was hampered by poor signal to noise necessitating use of L-FABP concentrations higher than the K_ds under study, limiting accurate measurement of the strongest affinities. It is thus not surprising that in general the affinities determined by intrinsic fluorescence were weaker than those determined by ANS displacement. In several cases, most notably

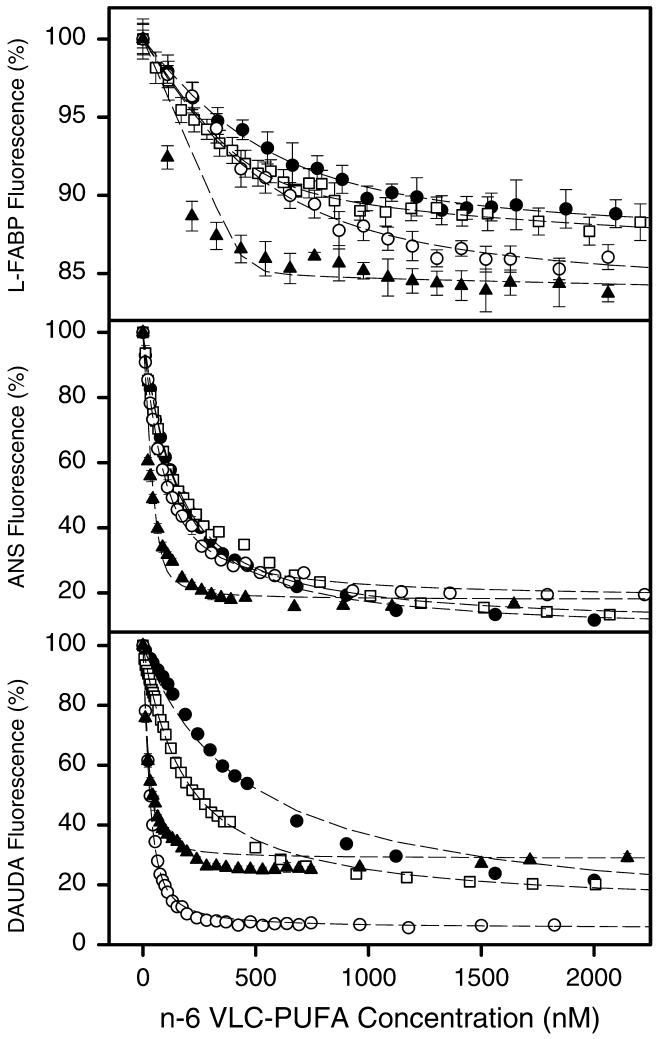

Fig. 7. Titration of L-FABP with n-6 VLC-PUFAs monitoring intrinsic fluorescence (top panel), displacement of ANS (middle panel), or displacement of DAUDA (bottom panel) upon titration with 20:4n-6 (closed circle), 22:4n-6 (open square), 24:4n-6 (open circle), and 24:5n-6 (closed triangle). Dashed lines represent nonlinear regression fits used to determine binding affinities. Bars show the standard error of the fluorescence measurement.

22:6n-3 and 24:5n-6, the affinity determined by intrinsic fluorescence was significantly stronger than that determined by ANS displacement. This likely is due to imperfect correction of higher levels of background fluorescence contaminant found in these two PUFA preparations. The intrinsic binding data was better fit by the two-site binding equation, likely representing a small degree of binding to the second site as expected under these conditions. Alternatively, this could represent improved fitting of imperfect background correction by use of a model with a larger number of parameters. It is possible that the contaminant fluorophore interacts with L-FABP such that simple subtractive correction of the background is not accurate.

L-FABP has been shown to bind two fatty acid molecules, one with high affinity and one with lower affinity (10, 15, 27). The present experiments were designed to measure only the affinity of the strong (presumably more physiologically relevant) site. In order to determine the stoichiometry properly, study of much higher protein concentrations would be required. Long-chain fatty acids are poorly soluble in aqueous solutions, and may not be freely monomeric possibly even at sub-micromolar concentrations (29). As noted for other hydrophobic compounds (24), there is potential for the solubility/aggregation dynamic of the fatty acid to influence binding curves. Therefore, we report the binding affinities as apparent (noted as K_d') to take this possibility into account.

TABLE 1. Comparison of metabolically equivalent n-3 and n-6 PUFA affinities for L-FABP[a]

n-3		n-6	
Ligand	K_d' (nM)	Ligand	K_d' (nM)
20:5n–3	200 (170–220)	20:4n–6	110 (105–120)
22:5n–3	67 (52–85)	22:4n–6	110 (100–130)
22:6n–3	140 (130–150)		
24:5n–3	66 (56–78)	24:4n–6	54 (50–59)
24:6n–3	180 (150–210)	24:5n–6	7 (2–14)

[a] Binding curves were generated by measurement of ANS displacement by PUFAs. Apparent dissociation constants were determined by non-linear regression of binding data to a one-site model. In parentheses are rigorous, support plane 95% confidence intervals generated from the regression analysis using Scientist.

Binding of n-3 and n-6 VLC-PUFA to L-FABP

We find that L-FABP binds a variety of 20, 22, and 24 carbon n-3 and n-6 VLC-PUFAs (Table 1). Affinities of 20:4n-6 for rat L-FABP have recently been determined at K_d = 48 nM (19) and 60–160 nM (18), with affinities for L-FABP from other species ranging 2–100 nM (15, 19), comparing well to our findings of K_d' = 110 nM. Affinities of 22:6n-3 for rat L-FABP have been reported at K_d = 23 nM (19), somewhat stronger binding than our finding of K_d' = 140 nM. The binding of 22:6n-3 to human L-FABP has been reported to have a K_i of 820 nM (17), weaker than our study. However, the K_is reported for L-FABP in that study tended to be weaker for nearly all fatty acids than recent work (15, 18, 19) would suggest. This group also found that 24:1n-9 bound well to human L-FABP compared with other fatty acids, with a K_i of 150 nM (17). We find no previous studies of FABP binding to the remaining seven VLC-PUFAs that we investigated.

The ability of L-FABP to bind 20:4n-6 and 22:6n-3 is not unique, as recently demonstrated in a study comparing fatty acid binding among a number of FABPs from other tissues (19). The affinity of 20:4n-6 for FABP from brain, myelin, heart, liver, intestine, and adipocyte ranged from 15–197 nM, with L-FABP in the middle of this range at 48–100 nM. The affinity of 22:6n-3 for these FABPs was more variable, ranging from 9–309 nM, with L-FABP again in the middle of the range at 19–23 nM.

Native L-FABP isolated from rat liver contains a variety of endogenous fatty acids from 16 to 22 carbons in length (12). The polyunsaturated fraction accounted for 44% of the total. Of the PUFA, 4% was n-3 and 96% was n-6. The only n-3 PUFA detected was 22:6n-3, but the n-3 PUFA dietary intake of these rats was not specified.

It is not surprising that L-FABP can accommodate PUFAs with chain lengths of 24 carbons because its binding cavity determined by X-ray crystallography is the largest of all studied FABPs (23) and it can accommodate a variety of hydrophobic ligands (10, 17). The lipid-binding pocket in the crystal structure contained two oleate molecules, with the inner fatty acid bound in a curved configuration. The inner binding site is most likely occupied first (23), and it is probably the high affinity site (10). It is difficult to predict from these studies if VLC-PUFAs are bound in the same configuration as oleate.

Possible role of L-FABP in n-3 VLC-PUFA processing

L-FABP has been shown to facilitate targeting of oleic acid (18:1n-9) for esterification into specific lipid pools (13). It is possible that L-FABP facilitates processing of VLC-PUFAs as well. In particular, n-3 PUFA processing from 18:3n-3 to 22:6n-3 involves intra-organelle trafficking on two occasions. The first is transport of 24:6n-3 from the endoplasmic reticulum to peroxisomes. Since L-FABP binds to 24:6n-3, it may facilitate the transport/targeting of 24:6n-3 to the peroxisome. Although there has been little investigation into the ability of L-FABP to deliver fatty acids to peroxisomes, one group found that 18:1n-9 and 16:0 (palmitic acid) bound to L-FABP are available to this organelle for metabolic processing (30). The second intra-organelle flux that occurs during n-3 VLC-PUFA metabolism is movement of 22:6n-3 back to the endoplasmic reticulum for esterification. Given that L-FABP binds 22:6n-3, it is possible that L-FABP also facilitates this flux.

Alternatively, it is possible that these n-3 VLC-PUFA intermediates are transported between organelles either in the unbound state or as their acyl CoA derivatives. Nonesterified fatty acids are able to desorb from lipid bilayers and diffuse through aqueous solution in the absence of binding protein (31, 32). The rate of spontaneous membrane desorption slows greatly as chain length increases, but is made faster by unsaturation (33). L-FABP has been shown to slow intermembrane diffusion of fatty acids in a cell-free model system (32), but also has been shown to increase cytoplasmic diffusion of fatty acids in cells (34, 35). A mathematical model has been formulated that predicts both possible behaviors (36).

There are several cytoplasmic proteins that bind fatty acyl CoAs. Acyl CoA binding protein binds 14–22 carbon fatty acyl CoA with K_d = 2–10 nM (37), and sterol carrier protein-2 binds 16–26 carbon fatty acyl CoA, with the highest affinities for 24 and 26 carbon fatty acyl CoA at IC_{50} = 100–440 nM (38). L-FABP also is capable of binding to fatty acyl CoAs as confirmed by several groups who report that the affinity of fatty acyl CoAs for L-FABP is stronger (39) or weaker (17, 27) than corresponding free fatty acids.

Differential processing of n-3 and n-6 VLC-PUFAs

Though n-6 PUFAs can proceed through the entire VLC-PUFA pathway from 18:2n-6 to 22:5n-6 via 24:5n-6, the biochemical process that causes the pathway to terminate primarily at 20:4n-6 under normal circumstances is not understood. The mechanism responsible for the differential processing of the n-6 as compared with n-3 PUFA could occur at the enzymatic level, or at the level of PUFA trafficking. Differences in L-FABP binding of n-3 and n-6 VLC-PUFAs could be an example of the latter. A number of mechanistic schemes involving L-FABP to effect differential processing of n-3 and n-6 PUFAs can be imagined. For example, one could postulate that if L-FABP strongly bound 20:4n-6 but not 20:5n-3, this could target the 20:4n-6 for esterification. Alternatively, one could postulate that L-FABP might have greater affinity for 24:6n-3 than 24:5n-6 and thereby facilitate the flux of 24:6n-3 but not 24:5n-6 to the peroxisome for further processing. We found only one striking difference in binding of parallel n-3 and n-6 VLC-PUFAs (Table 1): the much stronger binding of 24:5n-6 (K_d' = 7 nM) compared with 24:6n-3 (K_d' = 180 nM). Because of this, one could postulate that the strong binding of 24:5n-6 blocks the processing of n-6 VLC-PUFAs by serving as a sink, thus preventing further metabolism to 22:5n-6. However, if this is the case, one would expect to find high cellular levels of 24:5n-6, especially bound to L-FABP. This has not been observed (12), arguing against this possibility. Furthermore, the fluorescent background present in the 24:5n-6 preparation may have artifactually increased its apparent binding affinity.

Conclusions

We find that 20, 22, and 24 carbon n-3 and n-6 PUFAs bind to L-FABP with high affinity as determined by three fluorescence based assays. It is thus conceivable that L-FABP may modify the processing of these VLC-PUFAs. This may be especially important in 22:6n-3 synthesis from dietary PUFA precursors. However, there is little evidence on the basis of affinities that L-FABP is responsible for the differential processing of n-3 and n-6 VLC-PUFAs.

The authors thank Dr. Howard Sprecher for the kind gift of the 24 carbon PUFAs, Dr. Friedhelm Schroeder for the kind gift of L-FABP, and Richard Widstrom and Dr. David Hsu for helpful discussion. This work was supported by NIH grant HL49264 (A.A.S.) and by a Resident Research Grant from the American Academy of Pediatrics (A.W.N.).

Manuscript received 25 October 2001 and in revised form 28 January 2002.

REFERENCES

1. Sprecher, H. 2000. Metabolism of highly unsaturated n-3 and n-6 fatty acids. *Biochim. Biophys. Acta.* **1486:** 219–231.
2. Spector, A. A. 1999. Essentiality of fatty acids. *Lipids.* **34:** S1–S3.
3. Innis, S. M., H. Sprecher, D. Hachey, J. Edmond, and R. E. Anderson. 1999. Neonatal polyunsaturated fatty acid metabolism. *Lipids.* **34:** 139–149.
4. Connor, W. E., M. Neuringer, and S. Reisbick. 1992. Essential fatty acids: the importance of n-3 fatty acids in the retina and brain. *Nutr. Rev.* **50:** 21–29.
5. Uauy, R., E. Birch, D. Birch, and P. Peirano. 1992. Visual and brain function measurements in studies of n-3 fatty acid requirements of infants. *J. Pediatr.* **120:** S168–S180.
6. Martinez, M. 1996. Docosahexaenoic acid therapy in docosahexaenoic acid-deficient patients with disorders of peroxisomal biogenesis. *Lipids.* **31:** S145–S152.

7. Freedman, S. D., M. H. Katz, E. M. Parker, M. Laposata, M. Y. Urman, and J. G. Alvarez. 1999. A membrane lipid imbalance plays a role in the phenotypic expression of cystic fibrosis in cftr(−/−) mice. *Proc. Natl. Acad. Sci. USA*. **96:** 13995–14000.
8. de Urquiza, A. M., S. Liu, M. Sjöberg, R. H. Zetterström, W. Griffiths, J. Sjövall, and T. Perlmann. 2000. Docosahexaenoic acid, a ligand for the retinoid X receptor in mouse brain. *Science.* **290:** 2140–2144.
9. Gordon, J. I., D. H. Alpers, R. K. Ockner, and A. W. Strauss. 1983. The nucleotide sequence of rat liver fatty acid binding protein mRNA. *J. Biol. Chem.* **258:** 3356–3363.
10. Thompson, J., A. Reese-Wagoner, and L. Banaszak. 1999. Liver fatty acid binding protein: species variation and the accommodation of different ligands. *Biochim. Biophys. Acta.* **1441:** 117–130.
11. Ek, B. A., D. P. Cistola, J. A. Hamilton, T. L. Kaduce, and A. A. Spector. 1997. Fatty acid binding proteins reduce 15-lipoxygenase-induced oxygenation of linoleic acid and arachidonic acid. *Biochim. Biophys. Acta.* **1346:** 75–85.
12. Murphy, E. J., R. D. Edmondson, D. H. Russell, S. Colles, and F. Schroeder. 1999. Isolation and characterization of two distinct forms of liver fatty acid binding protein from the rat. *Biochim. Biophys. Acta.* **1436:** 413–425.
13. Murphy, E. J., D. R. Prows, J. R. Jefferson, and F. Schroeder. 1996. Liver fatty acid-binding protein expression in transfected fibroblasts stimulates fatty acid uptake and metabolism. *Biochim. Biophys. Acta.* **1301:** 191–198.
14. McArthur, M. J., B. P. Atshaves, A. Frolov, W. D. Foxworth, A. B. Kier, and F. Schroeder. 1999. Cellular uptake and intracellular trafficking of long chain fatty acids. *J. Lipid Res.* **40:** 1371–1383.
15. Wolfrum, C., T. Börchers, J. C. Sacchettini, and F. Spener. 2000. Binding of fatty acids and peroxisome proliferators to orthologous fatty acid binding proteins from human, murine, and bovine liver. *Biochemistry.* **39:** 1469–1474.
16. Lawrence, J. W., D. J. Kroll, and P. I. Eacho. 2000. Ligand-dependent interaction of hepatic fatty acid-binding protein with the nucleus. *J. Lipid Res.* **41:** 1390–1401.
17. Maatman, R. G., H. T. van Moerkerk, I. M. Nooren, E. J. van Zoelen, and J. H. Veerkamp. 1994. Expression of human liver fatty acid-binding protein in *Escherichia coli* and comparative analysis of its binding characteristics with muscle fatty acid-binding protein. *Biochim. Biophys. Acta.* **1214:** 1–10.
18. Widstrom, R. L., A. W. Norris, and A. A. Spector. 2001. Binding of cytochrome P450 monooxygenase and lipoxygenase pathway products by heart fatty acid-binding protein. *Biochemistry.* **40:** 1070–1076.
19. Richieri, G. V., R. T. Ogata, A. W. Zimmerman, J. H. Veerkamp, and A. M. Kleinfeld. 2000. Fatty acid binding proteins from different tissues show distinct patterns of fatty acid interactions. *Biochemistry.* **39:** 7197–7204.
20. Kane, C. D., and D. A. Bernlohr. 1996. A simple assay for intracellular lipid-binding proteins using displacement of 1-anilinonaphthalene 8-sulfonic acid. *Anal. Biochem.* **233:** 197–204.
21. Lowe, J. B., A. W. Strauss, and J. I. Gordon. 1984. Expression of a mammalian fatty acid-binding protein in *Escherichia coli*. *J. Biol. Chem.* **259:** 12696–12704.
22. Nemecz, G., T. Hubbell, J. R. Jefferson, J. B. Lowe, and F. Schroeder. 1991. Interaction of fatty acids with recombinant rat intestinal and liver fatty acid-binding proteins. *Arch. Biochem. Biophys.* **286:** 300–309.
23. Thompson, J., N. Winter, D. Terwey, J. Bratt, and L. Banaszak. 1997. The crystal structure of the liver fatty acid-binding protein. A complex with two bound oleates. *J. Biol. Chem.* **272:** 7140–7150.
24. Norris, A. W., L. Cheng, V. Giguère, M. Rosenberger, and E. Li. 1994. Measurement of subnanomolar retinoic acid binding affinities for cellular retinoic acid binding proteins by fluorometric titration. *Biochim. Biophys. Acta.* **1209:** 10–18.
25. Eftink, M. R. 1997. Fluorescence methods for studying equilibrium macromolecule-ligand interactions. *Methods Enzymol.* **278:** 221–257.
26. Hulme, E. C. 1999. Analysis of binding data. *Methods Mol. Biol.* **106:** 139–185.
27. Rolf, B., E. Oudenampsen-Krüger, T. Börchers, N. J. Faergeman, J. Knudsen, A. Lezius, and F. Spener. 1995. Analysis of the ligand binding properties of recombinant bovine liver-type fatty acid binding protein. *Biochim. Biophys. Acta.* **1259:** 245–253.
28. Douliez, J. P., T. Michon, and D. Marion. 2000. Steady-state tyrosine fluorescence to study the lipid-binding properties of a wheat non-specific lipid-transfer protein (nsLTP1). *Biochim. Biophys. Acta.* **1467:** 65–72.
29. Vorum, H., R. Brodersen, U. Kragh-Hansen, and A. O. Pedersen. 1992. Solubility of long-chain fatty acids in phosphate buffer at pH 7.4. *Biochim. Biophys. Acta.* **1126:** 135–142.
30. Reubsaet, F. A., J. H. Veerkamp, M. L. Bruckwilder, J. M. Trijbels, and L. A. Monnens. 1990. The involvement of fatty acid binding protein in peroxisomal fatty acid oxidation. *FEBS Lett.* **267:** 229–230.
31. Hamilton, J. A., R. A. Johnson, B. Corkey, and F. Kamp. 2001. Fatty acid transport: the diffusion mechanism in model and biological membranes. *J. Mol. Neurosci.* **16:** 99–108.
32. Zucker, S. D. 2001. Kinetic model of protein-mediated ligand transport: influence of soluble binding proteins on the intermembrane diffusion of a fluorescent fatty acid. *Biochemistry.* **40:** 977–986.
33. Pownall, H. J. 2001. Cellular transport of nonesterified fatty acids. *J. Mol. Neurosci.* **16:** 109–115.
34. Murphy, E. J. 1998. L-FABP and I-FABP expression increase NBD-stearate uptake and cytoplasmic diffusion in L cells. *Am. J. Physiol.* **275:** G244–G249.
35. Luxon, B. A. 1996. Inhibition of binding to fatty acid binding protein reduces the intracellular transport of fatty acids. *Am. J. Physiol.* **271:** G113–G120.
36. Weisiger, R. A., and S. D. Zucker. 2002. Transfer of fatty acids between intracellular membranes: roles of soluble binding proteins, distance, and time. *Am. J. Physiol.* **282:** G105–G115.
37. Kragelund, B. B., J. Knudsen, and F. M. Poulsen. 1999. Acyl-coenzyme A binding protein (ACBP). *Biochim. Biophys. Acta.* **1441:** 150–161.
38. Dansen, T. B., J. Westerman, F. S. Wouters, R. J. Wanders, A. van Hoek, T. W. Gadella, Jr., and K. W. Wirtz. 1999. High-affinity binding of very-long-chain fatty acyl-CoA esters to the peroxisomal non-specific lipid-transfer protein (sterol carrier protein-2). *Biochem. J.* **339:** 193–199.
39. Frolov, A., T. H. Cho, E. J. Murphy, and F. Schroeder. 1997. Isoforms of rat liver fatty acid binding protein differ in structure and affinity for fatty acids and fatty acyl CoAs. *Biochemistry.* **36:** 6545–6555.